Ubiquitination Events in the Regulation of a Paternally Supplied Toxin in *C. elegans*

By

Chelsea Nicole Campbell

A Thesis Submitted in Partial Fulfillment
of the Requirements for the Degree of Master of Science

Middle Tennessee State University

Summer 2020

Thesis Committee:

Dr. Lynn Boyd

Dr. David Nelson

Dr. Matthew Elrod-Erickson

ACKNOWLEDGEMENTS

I owe many thanks to my committee members for making this thesis possible. Dr. Boyd, thank you for this opportunity and for encouraging my growth as a scientist. I am so much more confident and have come such a long way since I first started in the lab. To my other committee members, Dr. Nelson and Dr. E, thank you both for all of your support and advice over the last few years. I'm so thankful to have had such a supportive committee during this journey.

Most importantly, I would like to thank my family. Sloan, you're the best brother and friend I could've asked for. Mom, you have been there for me through all of my ups and downs. You've always been my biggest supporter and I hope I made you proud. I couldn't have done this without you.

ABSTRACT

Successful development of an organism requires a highly complex coordination of various processes within the cell. The embryonic lethal toxin, PEEL-1, has been shown to disrupt early development in *C. elegans* and ultimately results in the death of the developing embryo without rescue by the antitoxin, ZEEL-1. Using a transgenic worm strain expressing PEEL-1::GFP, we have demonstrated the complete pathway through which PEEL-1 is ubiquitinated and degraded. The first step in ubiquitination is through the sole ubiquitin activating enzyme found in *C. elegans*, UBA-1. Using RNAi techniques, we then determined UBC-18 to be the conjugating enzyme responsible in the ubiquitin cascade. Subsequently, C17H11.4, C27A12.6, and HECD-1 work in coordination as ligation enzymes. With PEEL-1 being a transmembrane protein and inaccessible to the proteasome, we demonstrated that PEEL-1 is likely being degraded via autophagy. We also show that MO and PEEL-1 levels decrease throughout the one and two cell stages of early development. Finally, we found data that suggests that the increased lethality associated with *ubc-18* knockdown can be attributed to the persistence of PEEL-1.

TABLE OF CONTENTS

LIST OF FIGURES

LIST OF TABLES

LIST OF ABBREVIATIONS

GFP: green fluorescent protein

K48: lysine 48

MO: membranous organelles

NGM: nematode growth medium

RNAi: ribose nucleic acid interference

Ub: ubiquitin

UBC: ubiquitin conjugating enzyme

UPS: ubiquitin proteasome system

CHAPTER ONE: INTRODUCTION

Proper development of a multicellular organism depends on the coordination and regulation of numerous factors during embryogenesis. While some proteins may be necessary for proper development, others may be harmful to the developing organism. The ubiquitin proteasome system has shown the ability to regulate multiple processes during early development and plays a crucial role in cell cycle progression, cell fate determination, and degradation of damaged proteins. The degradation accomplished via ubiquitination is a key regulator in the creation of properly formed embryos (Bowerman and Kurz, 2006).

1.1 Ubiquitin Proteasome System

Ubiquitination is a reversible posttranslational modification that regulates numerous processes within the cell including marking proteins for proteasomal degradation. Ubiquitin is a 76 amino acid protein that is covalently attached to proteins forming mono or polyubiquitin chains. The process of ubiquitination involves the coordination of E1, E2, and E3 enzymes which leads to the attachment of ubiquitin to a substrate. An E1 activating enzyme first binds both ATP and ubiquitin to adenylate the C-terminal glycine of ubiquitin. A thioester bond is then formed between the E1 cysteine and a glycine on the now activated ubiquitin (Figure 1A) (Schulman and Harper, 2009). An E2 conjugating enzyme then catalyzes the transfer of ubiquitin from the E1 to a cysteine of the E2 via transthiolation (Figure 1B). In most cases, ubiquitin is then directly transferred from the E2 to the substrate through the formation of an isopeptide

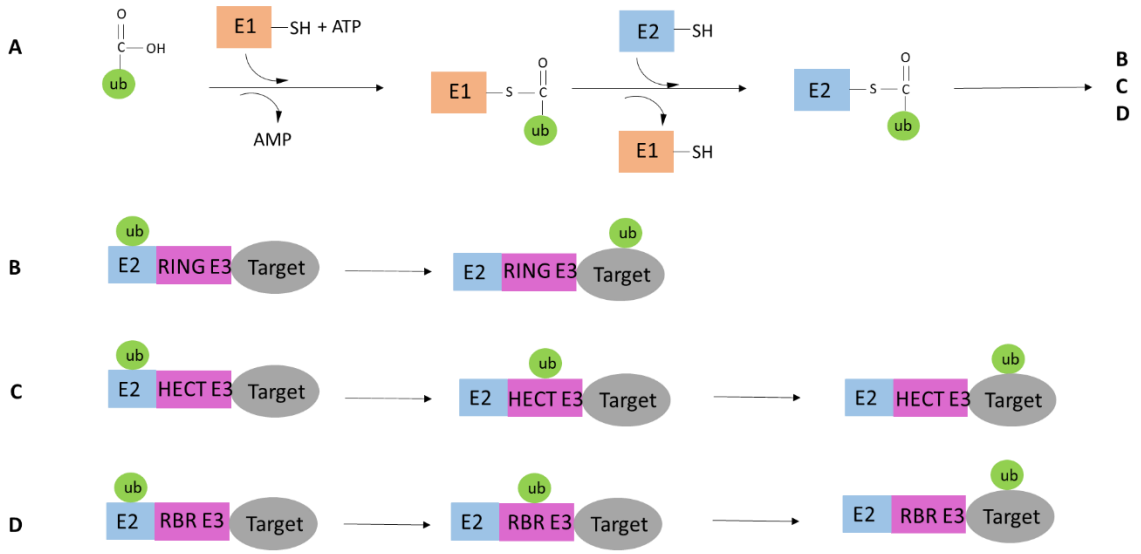

Figure 1: The process of ubiquitination

The addition of ubiquitin to a substrate involves the coordination of three enzymes. **(A)** The pathway begins with the "activation" of ubiquitin via the E1 activating enzyme and ATP. Ubiquitin is then transferred from the E1 to an E2 conjugating enzyme via transthiolation. Finally, ubiquitin is transferred to the target protein with an E3 ubiquitin ligase. **(B)** RING E3s allow for direct transfer of ubiquitin from the E2 to the target protein. **(C)** Ubiquitin is transferred from the E2 to the HECT E3. The ubiquitin is then transferred from the HECT to the target protein. **(D)** The E2 bound ubiquitin is recruited to the RING1 domain of the RBR. Ubiquitin is released from the E2 and transferred to the RING2 domain of the RBR. Finally, ubiquitin is transferred to the target protein.

bond with a lysine residue on the target protein. In an alternative method, the ubiquitin moiety is transferred from the E2 to an E3 forming a thioester bond. The E3 ubiquitin ligase then mediates the transfer of ubiquitin to the target protein by forming an isopeptide bond between a lysine of the protein and the C-terminal glycine of ubiquitin.

E3s are a diverse group of proteins and provide high substrate specificity during ubiquitination. Three families of E3s (RING, HECT, and RBR) catalyze the transfer of ubiquitin to the target protein through different mechanisms. RING family E3s function by bringing the E2 and substrate into close proximity and allow for the direct transfer of ubiquitin from the E2 to the substrate (Figure 1B). HECT E3s work by bringing the E2 bound ubiquitin to the E3 allowing the formation of a thioester bond between ubiquitin and the E3. The ubiquitin is then transferred from the E3 to the substrate (Figure 1C). RBR E3s (RING between RING) function as a HECT/RING hybrid by recruiting the E2 bound ubiquitin to the RING1 domain. Ubiquitin is then released from the E2 and is transferred to the RING2 domain of the E3. Finally, the ubiquitin is released from the E3 and noncovalently binds to the substrate (Figure 1D) (Yuan *et al*., 2017).

Ubiquitination can include the addition of one ubiquitin moiety to the substrate resulting in monoubiquitination. However, the 7 lysine residues and N-terminal methionine found in ubiquitin allow for additional ubiquitin molecules to be added to the ubiquitin on the target protein creating polyubiquitin chains (Sadowski *et al*., 2012). The formation of these polyubiquitin chains (K6, K11, K27, K29, K33, K48, K63, and M-1) provide the cell with different cues that determine the substrate's fate. One of the most characterized chains is the K48 chain, which generally targets proteins for proteasomal degradation

(Thrower *et al*., 2000). The 26S proteasome consists of a 19S regulatory particle, which caps the proteolytically active 20S core. The 19S cap functions to remove ubiquitin chains from the substrate, which are then fed to the 20S core to be degraded (Bard *et al.*, 2018). Despite signaling for proteasomal degradation, transmembrane proteins modified with K48 chains are not accessible to the proteasome and are therefore targeted for lysosomal degradation (MacGurn *et al*, 2012).

1.2 Toxin-Antitoxin Systems

Toxin-antitoxin (TA) systems consist of two closely linked genes that encode for a harmful toxin and a protective antitoxin (Melderen and De Bast, 2009). There are five classes of TA systems which are categorized according to the structure and relationship of the toxin and antitoxin. All five classes contain a protein toxin and an antitoxin that is either a protein or small RNA (sRNA). In Type I systems, the antitoxin sRNA prevents the translation of the toxin RNA. The most characterized system, Type II, consists of a protein antitoxin that binds and forms a protein-protein complex to inhibit the toxin. Type III TA systems have an antitoxin RNA that binds and inhibits the toxin. In Type IV TA systems, the toxin and antitoxin do not directly interact. The protein antitoxin interferes with the binding of the toxin to its target rather than direct binding as in the Type II system. Finally, Type V systems contain a protein antitoxin that prevents translation of the toxin (Unterholzner, 2013).

Many organisms have incorporated between one or dozens of TA systems into their genomes that typically function to regulate cell growth and death. The *Escherichia coli* genome, for example, contains 36 known TA systems (Yamaguchi and Inouye, 2011).

Often times these TA systems go undiscovered as their components frequently reach homeostasis in the population. In addition, some genes may appear to be essential for proper embryonic development while they actually function as an antitoxin to a hidden toxin. Such is the case with the *sup-35/pha-1* element in *C. elegans.* *pha-1* was originally hypothesized to be essential for pharyngeal development due to the defects seen in *pha-1* mutants (Mani and Fay, 2009). It has now been determined that PHA-1 is a zygotically expressed antitoxin to combat the maternally supplied toxin SUP-35 (Ben-David *et al*., 2017). SUP-35 appeared to be a target of ubiquitination and increased levels of SUP-35 were seen in *ubc-18* mutants. This finding suggests that the ubiquitin proteasome system may be involved in the regulation of this toxin. It is hypothesized that UBC-18 plays a role in regulating the stability and expression of SUP-35 to combat its toxicity to the embryo (Ben-David *et al.*, 2017).

TA systems are currently being explored as an option in controlling the spread of infectious diseases. One such case of this possibility can be seen in the intracellular bacteria *Wolbachia*. This bacterium typically infects arthropods and enhances its transmission through the female germline via cytoplasmic incompatibility caused by the cidA-cidB operon. Cytoplasmic incompatibility is characterized by the inability of sperm and egg to produce viable offspring. Infected sperm with the CidB enzyme are modified such that they cause embryonic lethality when fused with an uninfected egg not expressing CidA. In contrast, infected eggs fertilized by infected sperm are viable and develop normally (Beckmann *et al*, 2017). *Wolbachia* infection has been seen to reduce mosquito lifespan as well as inhibit transmission of pathogens. This phenotype associated with infection illustrates the potential use of *Wolbachia* in controlling

mosquito-borne disease via the introduction of infected mosquitos into the general population (Hancock *et al*, 2011).

1.3 The *peel-1/zeel-1* Element

Selfish genetic elements are elements that increase the rate of their own transmission relative to the rest of the genome although they may be neutral or harmful to an organism. These elements have been seen to influence many biological systems including development and evolution (Werren, 2011). One case of this phenomenon can be seen in the TA system known as the *peel-1/zeel-1* element in *C. elegans.* The *peel-1/zeel-1* (*paternal effect epistatic effect embryonic lethal-1/zygotic epistatic embryonic lethal*-1) element codes for a sperm supplied lethal toxin, PEEL-1, and a zygotically expressed antitoxin, ZEEL-1 (Seidel *et al*, 2011). When worms carrying the *peel-1/zeel-1* element are crossed with worms that do not carry it, all F1 worms still have *peel-1* and *zeel-1* expression. F2 generation worms all have sperm containing PEEL-1. However, 25% of the F2 generation does not zygotically express ZEEL-1, resulting in embryonic lethality (Figure 2A). Without rescue by the zygotically expressed ZEEL-1, these embryos fail to hatch.

Very little is known about PEEL-1 and the mechanism resulting in its toxicity to the developing embryo. PEEL-1 has been identified as a hydrophobic four pass transmembrane protein. PEEL-1 is exclusively expressed in sperm and localized to nematode specific membranous organelles (MOs) (Figure 2B). After being packaged into sperm, PEEL-1 is delivered to the embryo where it has lethal effects without rescue by the zygotically expressed ZEEL-1. ZEEL-1 is transiently expressed in the embryo

A

P1	$\frac{peel^+zeel^+}{peel^+zeel^+}$ x $\frac{peel^-zeel^-}{peel^-zeel^-}$
F1	$\frac{peel^+zeel^+}{peel^-zeel^-}$ 100%
F1 x F1	$\frac{peel^+zeel^+}{peel^-zeel^-}$ x $\frac{peel^+zeel^+}{peel^-zeel^-}$
F2	$\frac{peel^+zeel^+}{peel^+zeel^+}$ 25% 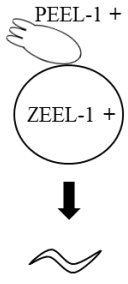 $\frac{peel^-zeel^-}{peel^-zeel^-}$ 25% 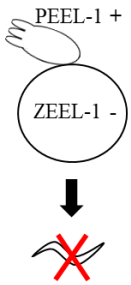 $\frac{peel^+zeel^+}{peel^-zeel^-}$ 50% 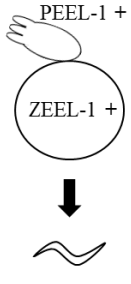

B

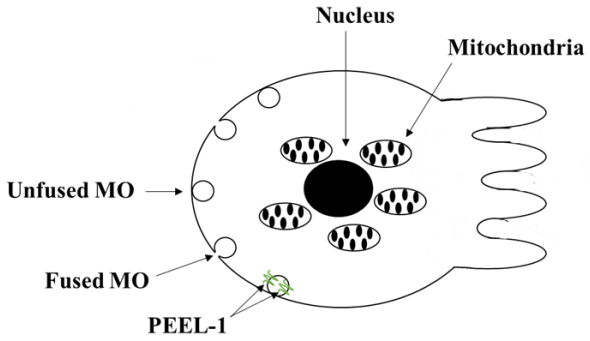

Figure 2: Graphic representation of the *peel-1/zeel-1* element

(A) Only the F2 generation of worms are affected with embryonic lethality. **(B)** The transmembrane protein, PEEL-1, localizes to sperm specific membranous organelles.

starting at eight cells and stops expression at approximately 150 cells (Seidel *et al*, 2011). Because PEEL-1 is localized to MOs and these organelles are typically degraded by eight cells, it appears that PEEL-1 and ZEEL-1 do not directly interact. It is possible that the *peel-1/zeel-1* element is a Type V TA system and the continued expression of ZEEL-1 works to prevent translation of PEEL-1.

Interestingly, the detrimental effects of PEEL-1 are not seen until the two-fold stage of development. Embryos effected by PEEL-1 appear to have normal morphogenesis throughout embryogenesis and gastrulation. Once reaching the two-fold stage, the embryo arrests and exhibits muscle and epidermal malfunction. These embryos appear to be paralyzed and never roll around within their eggshell, a result of a defect in muscle contraction. These effects are detrimental to the developing embryo and result in embryonic lethality (Seidel *et al*, 2011).

There is reason to believe that the UPS may be involved in the regulation of PEEL-1. It is known that PEEL-1 localizes to MOs, which are quickly ubiquitinated with K48 and K63 chains following fusion of oocyte and sperm (Hajjar *et al*, 2014). Knockdown of the ubiquitin conjugating enzyme *ubc-18* results in loss of K48 chains on MOs and stops proteasome recruitment (Molina *et al*, 2019). Another clue that the UPS may be involved regards *zeel-1*'s sequence similarity to *zyg-11*, a substrate recognition subunit to an E3 ubiquitin ligase (Seidel *et al*, 2008). With this knowledge, we hypothesize that the UPS may be involved in the regulation of PEEL-1.

1.4 Project Objectives and Summary

This study aimed to understand the possible involvement of the UPS in the regulation of the sperm supplied embryonic lethal protein, PEEL-1. Knockdown of the ubiquitin conjugating enzyme *ubc-18* resulted in a dramatic increase in persistence of PEEL-1. With this knowledge, an RNAi screen of 19 HECT and RBR E3 ligases was conducted to identify the E3 required for *ubc-18* dependent regulation of PEEL-1. This screen revealed 3 E3s that seem to be involved in the regulation of PEEL-1: 2 RBRs, C17H11.4 and C27A12.6, and the HECT *hecd-1*. To conclude the pathway of PEEL-1 regulation, embryos were subjected to *rad-23/rpn-10* knockdowns which suggested the lysosome to be the destination of PEEL-1. Antibody staining with the MO specific antibody, ICB4, shows decreased persistence of MOs and PEEL-1 through early stages of development. Finally, we show that PEEL-1 persistence is likely responsible for embryonic lethality associated with loss of *ubc-18*.

CHAPTER TWO: MATERIALS AND METHODS

2.1 *C. elegans* Strains and Maintenance

All *C. elegans* strains were maintained on nematode growth medium (NGM) plates containing .017 % agar, 0.003 % NaCl, and 0.0025 % peptone per liter. After the NGM solution was autoclaved and cooled, 0.001 % 1M $CaCl_2$, 0.001 % cholesterol (5 mg/mL), 0.001 % 1 M $MgSO_4$, and 0.025 % 1 M KPO_4 were added. 35 mm plates contained 5 mL of NGM and 60 mm plates contained 15 mL of NGM.

The OP50 strain of *E. coli* was streaked onto tryptic soy agar (TSA) and incubated at 37°C for 16 hours. A single colony of bacteria was then grown in a shaking incubator at 225 rpm in tryptic soy broth (TSB) at 37°C for 16 hours. 60 mm NGM plates were then seeded with 0.5 mL of OP50 culture. Finally, wild type N2 worms were grown at 20°C and the transgenic EG5766 strain was incubated at 25°C.

2.2 RNAi by Feeding

RNAi is a technique used to knockdown the expression of specific genes by feeding worms bacteria expressing dsRNA for each gene of interest. RNAi clones used in this study were obtained from the Ahringer Library or the Vidal ORF library. These RNAi clones were streaked from glycerol stocks onto TSA containing ampicillin (100 µg/mL) and tetracycline (10 µg/mL) and incubated overnight. A single colony was selected and grown in a shaking incubator at 225 rpm for 16 hours at 37°C in TSB containing ampicillin (100 µg/mL) and tetracycline (10 µg/mL). The bacterial culture containing the dsRNA of interest was then seeded on NGM plates containing ampicillin (100 µg/mL)

and 0.2 % lactose. Simultaneous knockdowns were performed using a 1:1 mixture of each bacterial culture for different genes of interest. L4 worms were picked and placed on these plates and grown for 48 hours at the appropriate temperature. Controls used for RNAi experiments included the L4440 plasmid (vector) with no gene insertion in the HT115 bacterial strain serving as a negative control as well as the embryonic lethal gene, *ubc-2*, as a positive control.

2.3 Antibodies

The primary antibody used in this study was mouse monoclonal anti-1CB4 (generous gift from Dr. Steve L'Hernault, Emory University) used at 1:100 dilution. The secondary antibody used for immunofluorescence at 1:100 dilution was goat anti-mouse TRITC (Jackson ImmunoResearch Laboratories).

2.4 Antibody Staining

Two-day adults were placed on a cover slip in a drop of egg buffer containing a 1:20 dilution of 0.1mg/mL tetramisole (0.05 mg/mL). Worms were cut open with a needle to extract embryos and were then placed on poly-L-lysine coated slides. Slides were placed in liquid nitrogen for 5 minutes and the cover slip was removed before fixing slides in methanol for 20 minutes at -20°C. Slides were then washed 3 times in PBST (PBS with 0.5% Tween-20) for 5 minutes each. Slides were blocked with 30% goat serum in PBST for 60 minutes at room temperature, incubated with primary antibody (1:100) overnight at 4°C, and then incubated with secondary antibody (1:100) for 2 hours at room temperature. Three washes in PBST were performed after each stain. Finally,

Vectashield plus DAPI (Vector Labs, Burlingame, CA) was used to mount each sample before visualization via confocal microscopy.

2.5 Generation of *peel-1* RNAi Clone

The *peel-1* RNAi clone was generated in the L4440 plasmid using ligation independent cloning (Figure 3). The pL4440GTWY plasmid was streaked onto TSA plates containing ampicillin (100 µg/mL) and grown overnight. A single colony was picked and grown in 5 mL of TSB with ampicillin at 37°C for 16 hours shaking at 225 rpm. Miniprep purification was then performed using a Qiagen QIAprep Spin Miniprep Kit. Next, the plasmid was cut with NotI-HF and HindIII-HF (NewEngland Biolabs) to allow for the insertion of *peel-1*. Amplification of *peel-1* using whole worm genomic DNA was achieved through PCR using primers designed with SnapGene. Primers were obtained through Eurofin Genomics and are listed in Table 1.

Forward	ACATAATACTGTAAAACACAACATATCCAGTCACTATGGCATTTC CAAAACTTAAAATTTTCGATGATTTTCATATTTTTGTGG
Reverse	TTGGGTACCGGGCCCCCCCTCGAGGTCGACGGTATCGATATATTC TGGCATGGGTCAATGTAAAGGAC

Table 1: Primers used for amplification of *peel-1*.

The PCR product was purified using a Qiagen QIA quick PCR Purification Kit. The PCR insert was recombined into the pL4440GTWY plasmid by incubating 1 µL of digestion, 4 µL of purified PCR product, 5 µL of NEBuilder HiFi DNA Assembly Master Mix, and 1 µL of water at 50 °C for one hour. The plasmid was then transformed into NEB competent cells which were then grown on TSA containing ampicillin. A single colony was grown shaking at 225 rpm in 5 mL of TSB at 37°C for 16 hours. Miniprep purification was performed to extract the plasmid from the bacteria. Finally, the plasmid

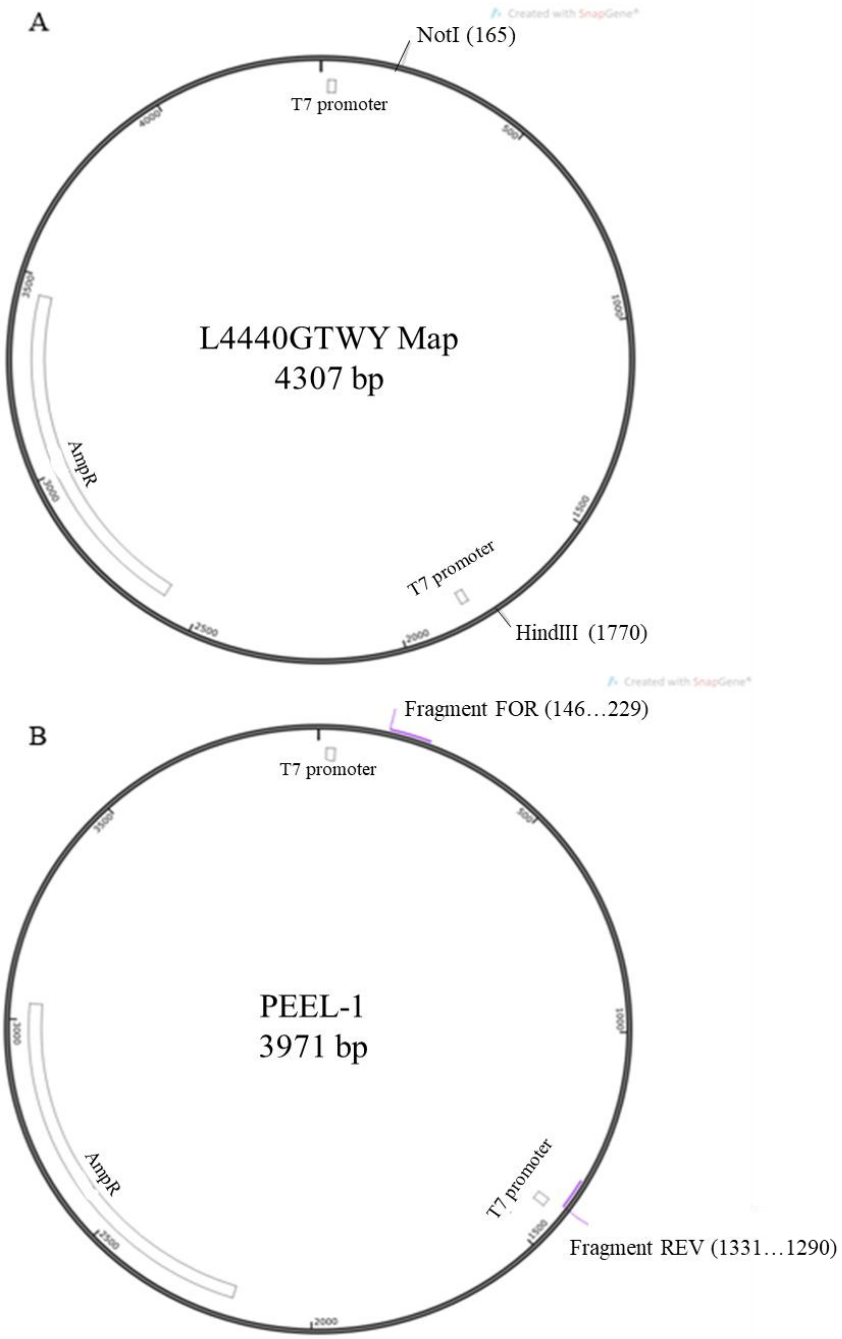

Figure 3: Creation of *peel-1* RNAi clone

(A) The L4440 plasmid contains an ampicillin resistant gene and restriction sites for NotI and HindIII, which were utilized for cloning. **(B**) Assembled plasmid containing *peel-1*.

was transformed into HT115 *E. coli* and grown on TSA containing ampicillin and tetracycline. A single colony was grown shaking at 225 rpm in 5 mL of TSB at 37°C for 16 hours. A frozen glycerol stock was prepared using 500 µL of bacterial culture and 500 µL of 50% glycerol. Proper construction of the *peel-1* RNAi clone was verified with DNA sequencing via Eurofins Genomics using the primers listed in Table 2.

M13F	TGT AAA ACG ACG GCC AGT
VR	ATT ACC GCC TTT GAG TGA GC

Table 2: Primers used for DNA sequencing of the *peel-1* RNAi clone.

2.6 Embryonic Lethality Assay

L4 hermaphrodites were placed on NGM RNAi plates with 5 treatment groups: vector, *ubc-2, ubc-18, peel-1, and peel-1*/*ubc-18*. L4 F1 progeny were then singled onto new plates, removed after 24 hours, and total number of eggs laid were counted. Hatched progeny were counted 48 hours after the worm was removed. Embryonic lethality was calculated by comparing the total number of hatched progeny after 48 hours to the total number of eggs laid.

2.7 Confocal Microscopy

All fluorescent images were obtained using a Zeiss LSM 700 confocal microscope equipped with Zen Black Software (Carl Zeiss). For live cell and antibody staining experiments, the 408 nm laser was used for DAPI, the 488 nm laser was used for GFP, and the 555 nm laser was used for TRITC. Image settings were kept constant for each set of experiments. All images throughout this thesis are maximum intensity z projections.

2.8 Statistical Analysis

Each figure legend indicates statistical tests performed and sample sizes for each experiment. Two tailed z tests were calculated using VassarStats. Fisher's exact test used in the embryonic lethality assay was conducted using GraphPad. Error bars represent 95% confidence intervals using the modified Wald method from GraphPad.

CHAPTER THREE: RESULTS

3.1 *ubc-18* knockdown results in persistence of PEEL-1::GFP

Following the fusion of the sperm and oocyte, the sperm supplied membranous organelles (MOs) become ubiquitinated with K48 and K63 chains. There is evidence that the ubiquitin conjugating enzyme *ubc-18* is responsible for the addition of K48 chains on MOs following fertilization (Molina *et al,* 2019). With this in mind, we hypothesized that *ubc-18* could potentially be involved in the regulation of PEEL-1. A transgenic worm expressing GFP tagged PEEL-1 was used to visualize the presence of PEEL-1 in the embryo following knockdown of *ubc-18.* RNAi knockdowns by feeding were performed according to Figure 4. Controls for all RNAi treatments included the L4440 plasmid vector with no gene insertion in the HT115 bacterial strain serving as a negative control, as well as L4440 containing the embryonic lethal *ubc-2* as a positive control. Treated embryos were visualized via confocal microscopy and representative embryos are shown in Figure 5A. PEEL-1 has previously been shown to colocalize to MOs in sperm and can be seen as distinct puncta in the embryo. Data shows persistence of PEEL-1::GFP in 23.7% (n=76) of vector treated embryos while *ubc-18* knockdown embryos showed 58% (n=62) (Figure 5B). These data suggest that PEEL-1::GFP persists in the embryo in the absence of UBC-18. This may indicate that PEEL-1 degradation following fertilization is regulated by UBC-18.

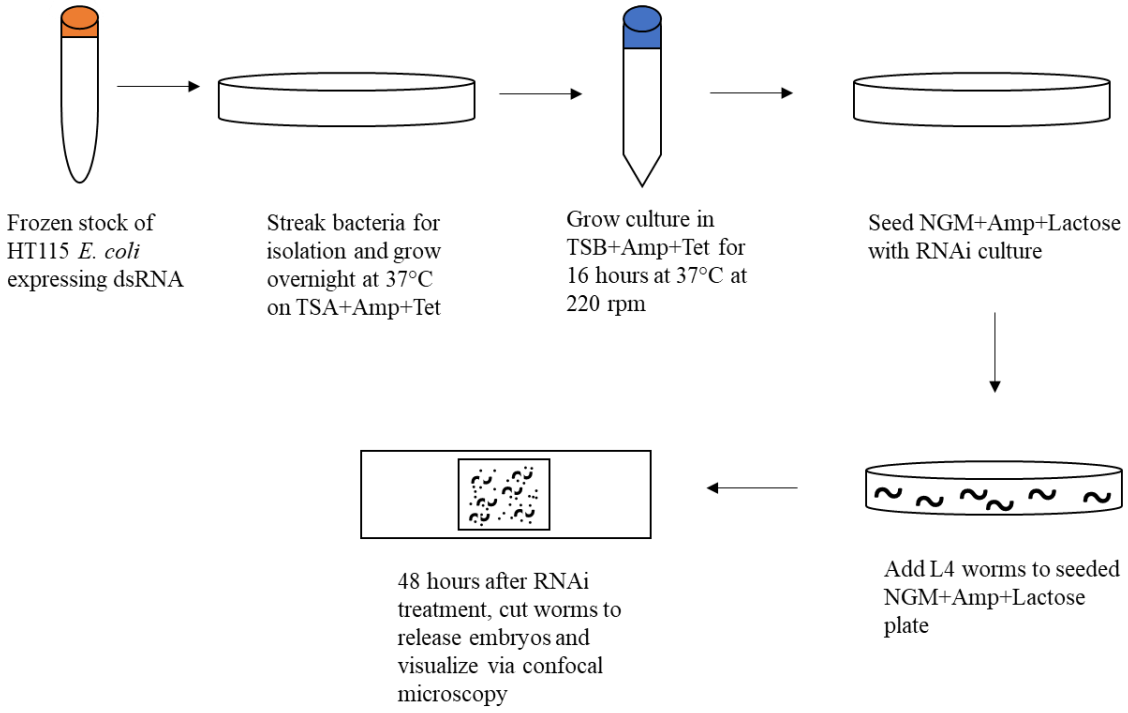

Figure 4: Experimental design for RNAi knockdowns by feeding

All knockdowns were performed using HT115 *E. coli* expressing dsRNA for the gene of interest. Controls for all experiments included the empty L4440 vector as a negative control and the embryonic lethal gene, *ubc-2*, as a positive control.

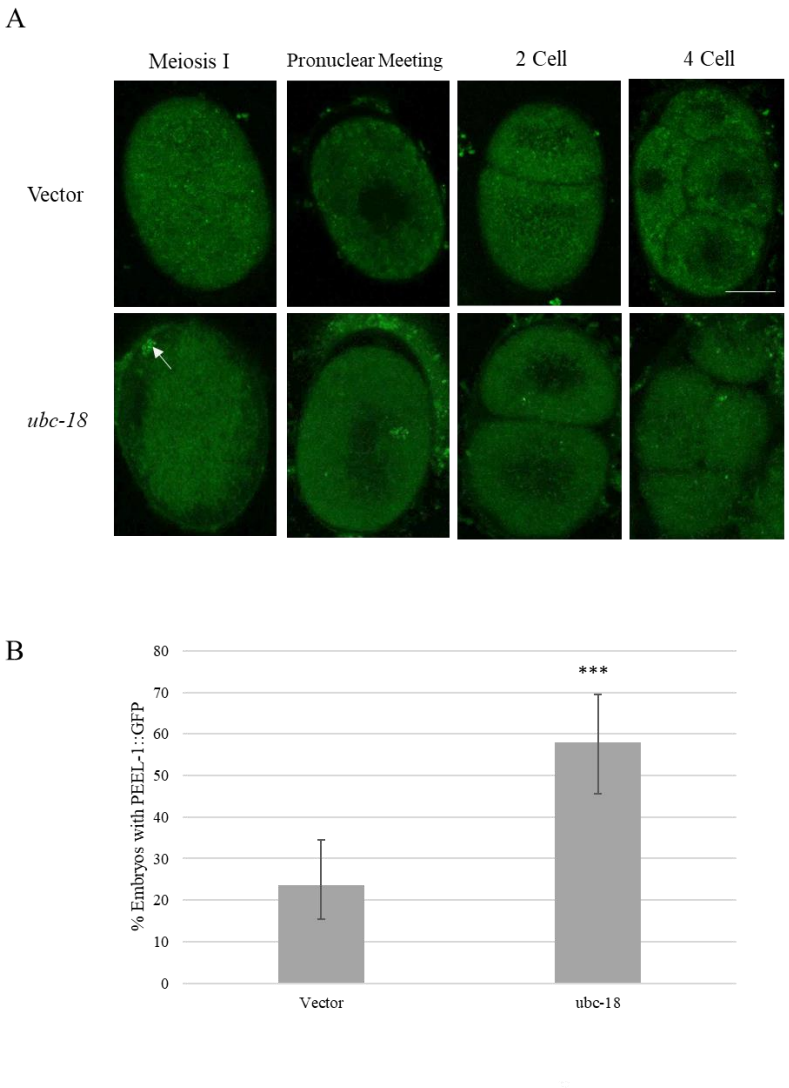

Figure 5: UBC-18 is involved in the degradation of PEEL-1 in embryos

(A) PEEL-1 localizes to MOs during embryogenesis. Representative embryos show puncta (arrows) indicating persistence of PEEL-1::GFP. **(B)** Visualization of embryos via confocal microscopy shows persistence of PEEL-1 in 23.68% of vector embryos (n=76) and 58.06% of *ubc-18* knockdown embryos (n=62). Statistical differences were determined using a two tailed z test with ***p<0.001. Error bars represent 95% confidence intervals. Scale bar represents 10 µm.

3.2 3 E3 ubiquitin ligases function with *ubc-18* in the regulation of PEEL-1

Human UBCH7, a conserved ortholog of *C. elegans ubc-18*, has been shown to exhibit exclusive reactivity with HECT and RBR E3s (Wenzel, *et al.* 2011). Therefore, upon establishing *ubc-18* as the E2 involved in the degradation of PEEL-1, a screen containing 19 HECT and RBR ubiquitin ligases was designed to determine the interacting E3 ubiquitin ligase. Using the same RNAi method as previously described in Figure 3, we determined the percentage of PEEL-1::GFP persistence in embryos following knockdown of each E3. *ubc-18* knockdown showed PEEL-1 persistence in more than 50% of embryos, so this was established as the cut off for "hits" in the screen.

Of 19 E3s tested (Figure 6A), 3 showed persistence of PEEL-1::GFP above the 50% cutoff: C17H11.4, C27A12.6, and *hecd-1*. Because multiple hits were found, these E3s were subjected to combination knockouts to determine the extent of their involvement in the regulation of PEEL-1. Results of the combination knockouts (Figure 6B) show that loss of all 3 E3s results in PEEL-1::GFP persistence in 55% of embryos. There is no statistical difference between the single and combination knockdowns which suggests that each E3 is equally important in the regulation of PEEL-1.

3.3 PEEL-1 degradation is likely accomplished via autophagy

After determining the E2 and E3s involved in regulating PEEL-1, we wished to identify the final step in the degradation of PEEL-1. Because PEEL-1 is a transmembrane protein, it cannot be targeted by the proteasome and is therefore likely targeted for autophagy and subsequently degraded in the lysosome. To test this, two proteasomal subunits, RAD-23 and RPN-10, were knocked down and persistence of PEEL-1::GFP

was observed via confocal microscopy (Figure 7A). Data showed no statistical significance between vector and *rad-23/rpn-10* treated embryos (Figure 7B), supporting our hypothesis that PEEL-1 is not degraded via the proteasome.

3.4 MO and PEEL-1 persistence decreases during early development

Previous studies have shown that ubiquitination is essential for removal of MOs in early stages of development (Molina *et al*., 2019). PEEL-1 localizes to MOs which are rapidly degraded following fertilization. With MOs and PEEL-1 both requiring ubiquitination, we wanted to determine whether decreased ubiquitination via *ubc-18* specifically stabilizes PEEL-1 or inhibits degradation of MOs. Embryos were treated and stained with the MO specific antibody, 1CB4. Persistence of MOs and PEEL-1 were visualized via confocal microscopy (Figure 8A). Data show that the mean number of MOs per embryo decreases from the one cell to two cell stage (Figure 8B). With PEEL-1 localizing to MOs, data also show the mean number of PEEL-1 positive MOs decreasing through one and two cell stage embryos well (Figure 7C). While both of these numbers decrease through these first few cell stages of development, an unpaired t test shows no statistical significance between vector and *ubc-18* treatment groups. This suggests that *ubc-18* is stabilizing PEEL-1 in the embryo.

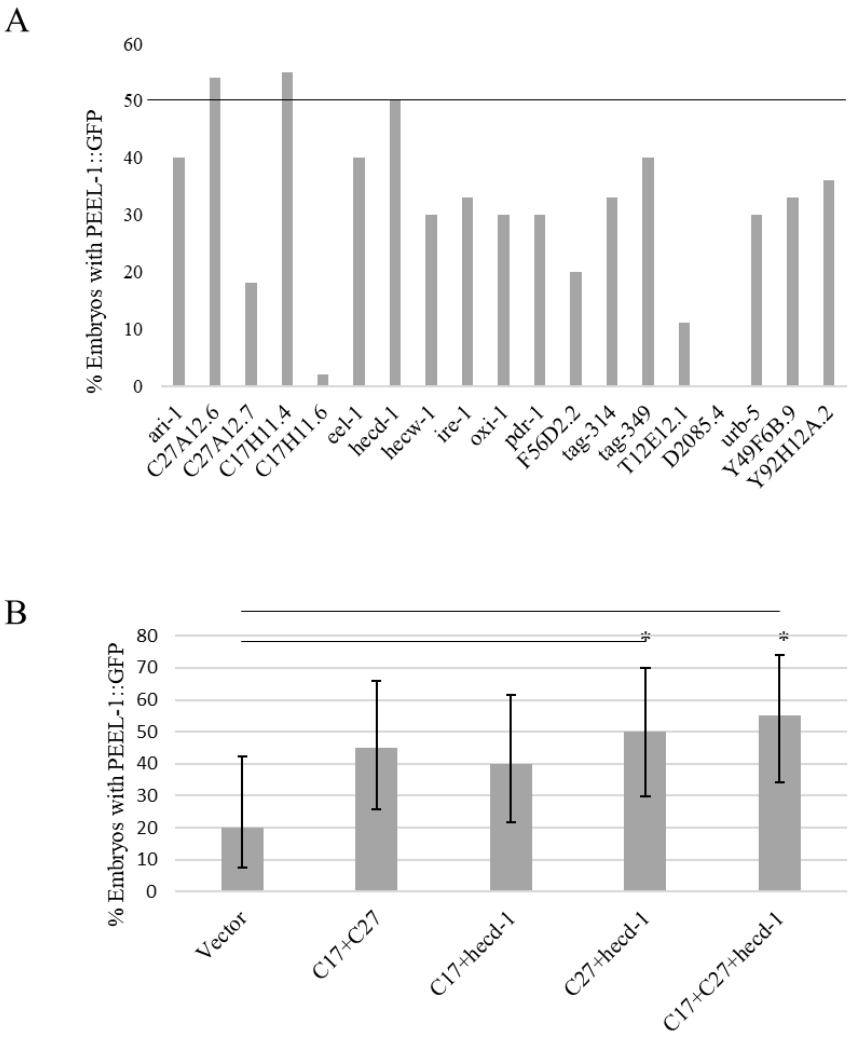

Figure 6: 3 E3s are specifically involved in the regulation of PEEL-1

(A) 10 embryos were counted for each of 19 knockdowns in the E3 screen. C17H11.4, C27A12.6, and *hecd-1* each showed persistence of PEEL-1::GFP above the 50% cutoff and were then subjected to combination knockouts. **(B)** 20 embryos were observed for each condition. Statistical differences were calculated with a two tailed z test with *$p<0.05$. Error bars represent 95% confidence intervals.

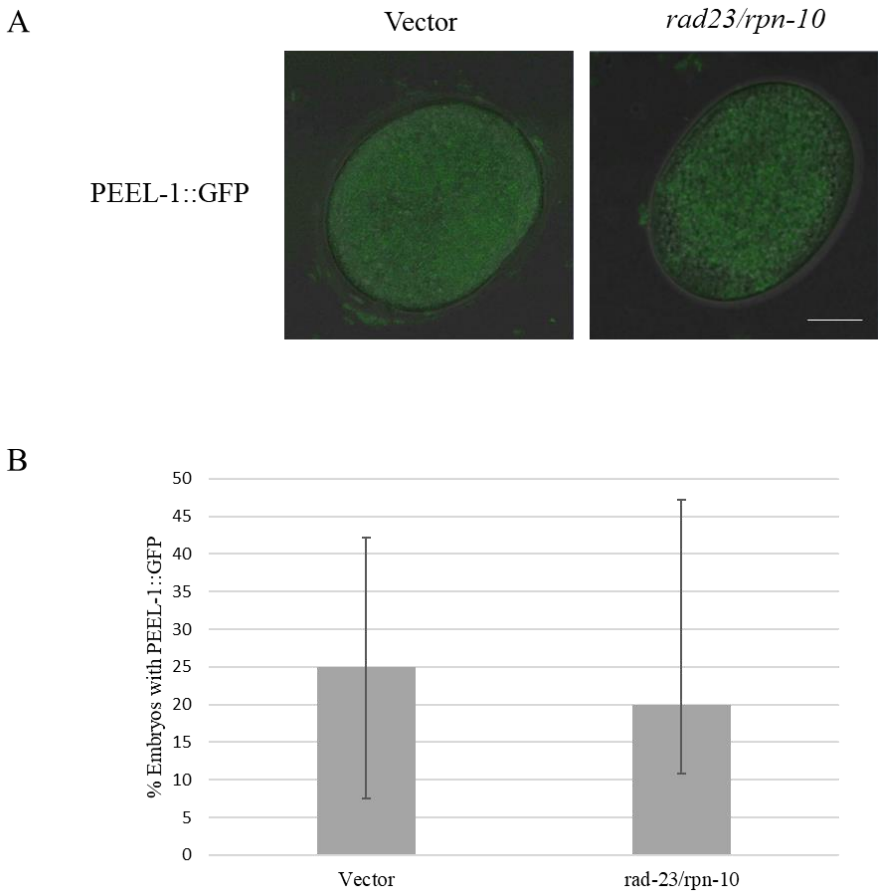

Figure 7: Proteasome knockdown does not increase PEEL-1 persistence

(A) Representative meiosis stage embryos show no persistence of PEEL-1::GFP in *rad-23/rpn-10* treated embryos. **(B)** 20 embryos were observed for each condition and statistical differences were calculated with a two tailed z test. Differences between vector and *rad-23/rpn-10* treated embryos are not statistically significant. Error bars represent 95% confidence intervals. Scale bar represents 10 µm.

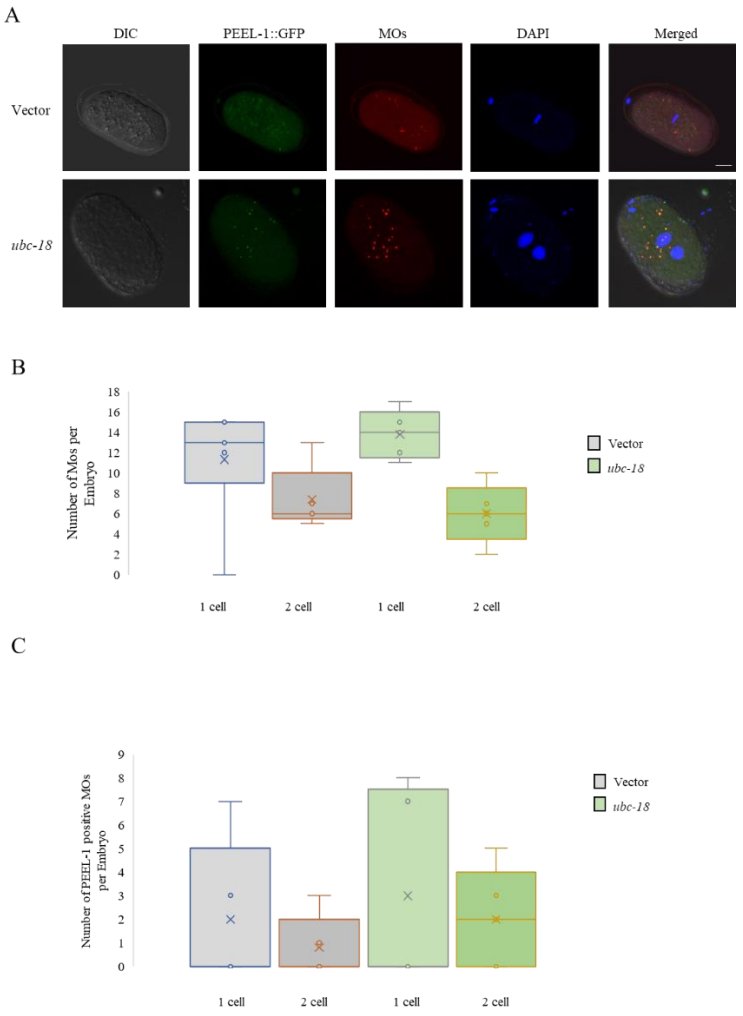

Figure 8: Number of PEEL-1 positive MOs decreases in early development

(A) Representative one cell stage embryos show colocalization of MOs and PEEL-1. **(B)** The mean number of MOs decline through development; however there does not appear to be a difference between vector and *ubc-18* embryos in the one and two cell stage. **(C)** The mean number of PEEL-1 positive MOs also decreases through development showing no significance between treatment groups. The number of MOs were counted in 5 embryos for each treatment group. Statistical significance was determined by an unpaired t test and scale bar represents 10 µm.

3.5 Embryonic lethality associated with *ubc-18* is a result of PEEL-1 persistence

While *ubc-18* is involved in the addition of K48 chains on MOs, loss of this enzyme also results in decreased embryonic viability with about 30% of embryos not hatching (Molina *et al*., 2019). With embryonic lethality also associated with PEEL-1, the question arises if lethality is a result of loss of *ubc-18* or persistence of PEEL-1. To determine this, a *peel-1* RNAi clone was generated in the L4440 plasmid (Figure 8) and verified with DNA sequencing. Knockdown of *peel-1* showed loss of GFP signal in worms expressing PEEL-1::GFP. L4 worms were then subjected to various knockdowns including a combination with *ubc-18/peel-1*, and the F2 hatching percentage was calculated. Knockdown of *peel-1* alone shows no embryonic lethality, consistent with vector treated embryos. Data show that simultaneous knockdown of *ubc-18/peel-1* rescues lethality associated with *ubc-18* knockdown (Figure 9). With *ubc-18* knockdown resulting in embryonic lethality and persistence of PEEL-1, the rescue seen in the double knockdown suggests that embryonic lethality from *ubc-18* loss can be largely explained by the persistence of PEEL-1.

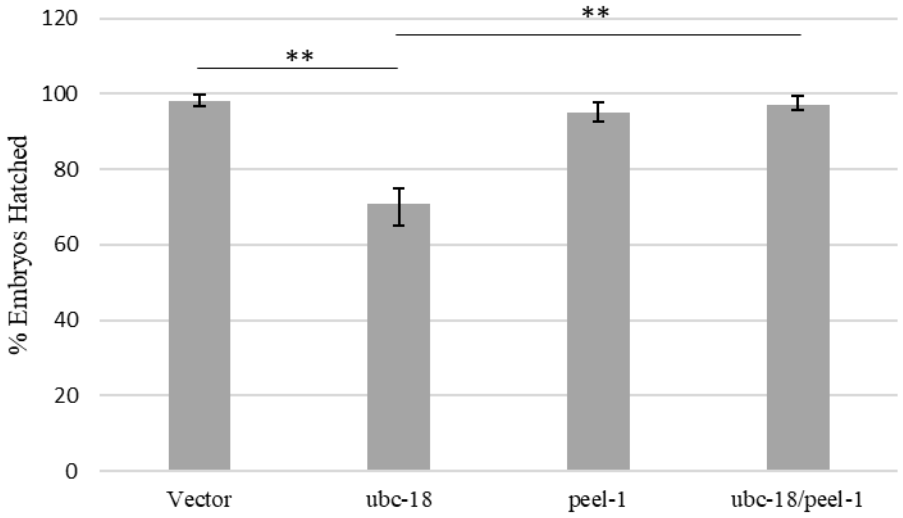

Figure 9: Knockdown of *peel-1* rescues embryonic lethality

Embryonic lethality was accessed for each condition with the following embryo counts: vector: 281, *ubc-18*: 329, *peel-1*: 267, and *ubc-18/peel-1*: 289. Knockdown of *ubc-18* results in embryonic lethality far greater than *ubc-18/peel-1* knockdown. Statistical differences between each treatment group were calculated with Fisher's exact test with **$p<0.001$ and error bars represent 95% confidence intervals.

CHAPTER FOUR: DISCUSSION

Very little work has been done to elucidate the mechanisms at play in the *peel-1/zeel-1* element. Although the proteins have been partially characterized, there is limited information characterizing PEEL-1 and how it interacts with the developing embryo, ultimately resulting in lethality. The goal of this study was to determine the possible role of ubiquitination in the regulation of PEEL-1 following fertilization. Here, we have determined the pathway through which PEEL-1 is being ubiquitinated and ultimately degraded. We have also provided evidence that lethality associated with loss of *ubc-18* is the result of persistence of PEEL-1. Understanding the mechanisms behind the *peel-1/zeel-1* element could ultimately lead to its use in population control, as seen in other toxin-antitoxin systems.

4.1 Ubiquitination and degradation of PEEL-1

Despite knowing very little about PEEL-1, we had various reasons to suspect the involvement of the UPS in the regulation of the lethal protein. Our results indicate that PEEL-1 is, in fact, regulated via ubiquitination. Although previous studies were not able to visualize PEEL-1 following fertilization (Seidel *et al,* 2011), we were able to detect PEEL-1::GFP in both live and fixed cells. Knockdown of *ubc-18* resulted in a significant increase in persistence of PEEL-1::GFP puncta in early stage embryos. Distinct puncta of PEEL-1::GFP could be visualized in one cell through four cell stage embryos but the GFP signal was too diffuse to be seen in later stages of development. This lack of GFP signal is likely the result of large amounts of PEEL-1 being rapidly degraded.

We also identified three ubiquitin ligases that are implicated in the regulation of PEEL-1. C17H11.4, C27A12.6, and *hecd-1* knockdowns all showed increased persistence of PEEL-1::GFP in the early embryo. Combination knockdowns of these E3s all showed consistent increased puncta of PEEL-1::GFP. One of the E3s involved, C27A12.6, is hypothesized to be involved in the development of muscle cells (Poush *et al*, 2018), and effects of PEEL-1 toxicity include defects in muscle contraction (Seidel *et al*, 2011).

Due to the transmembrane property of PEEL-1, we hypothesized that the proteasome could not be the final site of degradation for PEEL-1. The use of proteasome inhibitors can create multiple downstream effects, so we chose to knockdown two proteasomal subunits, *rad-23* and *rpn-10* to test this hypothesis. We saw no significant difference in persistence of PEEL-1::GFP in vector and *rad-23/rpn-10* treated embryos, which is consistent with the belief that the proteasome is not involved in the degradation of PEEL-1. With this finding in mind, we believe that ubiquitination of PEEL-1 ultimately leads to degradation via the autophagosome. To test this hypothesis, future studies could include knockdown of *lgg-1/lgg-2* which are essential for selective autophagy (Wu *et al*, 2015).

4.2 Persistence of MOs and PEEL-1

It has been shown that *ubc-18* responsible for the addition of K48 chains on MOs and knockdown of *ubc-18* results in persistence of MOs in the embryo (Molina *et al*, 2019). Our data is consistent with the finding that the mean number of MOs is reduced through development. However, we see no significant difference between vector and *ubc-18* treated embryos. While there is no statistical significance in the number of PEEL-1

positive MOs between treatment groups, there is a clear trend showing *ubc-18* knockdown embryos to have more PEEL-1 positive MOs. This lack of significance is possibly due to a small sample size because of time constraints. Ideally, we would like to have two to three times as many embryos in each treatment group to further investigate whether decreased ubiquitination is preventing degradation of PEEL-1 or if stabilization of MOs allows for persistence of PEEL-1.

4.3 PEEL-1 embryonic lethality

PEEL-1 has been shown to have lethal effects on the developing embryo without rescue by the zygotic antitoxin, ZEEL-1 (Seidel *et al,* 2008). Interestingly, loss of *ubc-18,* which we have shown to be involved in the regulation of PEEL-1, is also associated with low rates of embryonic lethality (Molina *et al,* 2019). We hypothesized that this lethality was due to persistence of PEEL-1 and that knockdown of *ubc-18/peel-1* would rescue this lethality. In fact, our data shows a significant increase in embryonic viability in the *ubc-18/peel-1* treatment group. This is a very exciting results and potentially explains why loss of *ubc-18* results in lethality.

Overall, our studies implicate the involvement of ubiquitin in the regulation of the paternally supplied toxin, PEEL-1. We have shown that the ubiquitination of PEEL-1 involves the coordination of *ubc-18* as well as three E3s: C17H11.4, C27A12.6, and *hecd-1*. We also have data supporting the hypothesis that the destruction of PEEL-1 ultimately occurs via autophagy. The number of MOs as well as number of PEEL-1 positive MOs decreases through early development; however, we see no significant difference in *ubc-18* embryos, likely due to small sample size. Finally, we show data that

suggests that embryonic lethality associated with loss of *ubc-18* is correlated to persistence of PEEL-1. Although we have just scratched the surface of how PEEL-1 is regulated, there is still much work needed in order to better understand PEEL-1, the method of its toxicity, and how it interacts with its antitoxin counterpart, ZEEL-1.

Literature Cited

Bard, J. *et al*. The 26S Proteasome Utilizes a Kinetic Gateway to Prioritize Substrate Degradation. *Cell* 177, 286–298 (2018).

Beckmann, J. *et al*. A Wolbachia deubiquitylating enzyme induces cytoplasmic incompatibility. *Nature Microbiology* 2, 1-7 (2017).

Ben-David, E. *et al*. A maternal-effect selfish genetic element in Caenorhaditis elegans. *Science* 356, 1051-1055 (2017).

Bowerman, B. and Kurz, T. Degrade to create: developmental requirement for ubiquitin-mediated proteolysis during early C. elegans embryogenesis. *Development* 133, 773-784 (2006).

Hajjar, C. *et al*. Dual roles for ubiquitination in the processing of sperm organelles after fertilization. *BMC Developmental Biology* 14, 1–11 (2014).

Hancock, P. *et al*. Strategies for Introducing Wolbachia to Reduce Transmission of Mosquito-Born Diseases. *PLoS Neglected Tropical Diseases* 5, 1-10 (2011).

MacGurn, J. *et al*. Ubiquitin and Membrane Protein Turnover: From Cradle to Grave. *Annual Review of Biochemistry* 81, 231-259. (2012).

Mani, K. and Fay, D. A Mechanistic Basis for the Coordinated Regulation of Pharyngeal Morphogenesis in Caenorhabditis elegans by LIN-35/Rb and UBC-18-ARI-1. *PLoS Genetics* 5, 1-16 (2009).

Melderen, L. and De Base, M. Bacterial Toxin-Antitoxin Systems: More Than Selfish Entities*? PLoS Genetics* 5, 1-6 (2009).

Molina, P. *et al*. Ubiquitination is required for the initial removal of paternal organelles in C. elegans. *Dev Biol*. 453(2): 168–179 (2019).

Poush, J. *et al*. Regulation of germ cell development by ARI1 family ubiquitin ligases in C. elegans. *Sci Rep.* 8, 1-12. (2018).

Sadowski, M. *et al*. Protein monoubiquitination and polyubiquitination generate structural diversity to control distinct biological processes. *IUBMB Life* 64, 136-142. (2012).

Schulman, B. and Harper, W. Ubiquitin-like protein activation by E1 enzymes: the apex for downstream signaling pathways. *Nature Reviews Molecular Cell Biology* 40, 319-331 (2009)

Seidel, H. *et al*. A Novel Sperm-Delivered Toxin Causes Late-Stage Embryo Lethality and Transmission Ratio Distortion in C. elegans. *PLoS Biology* 9 (2011).

Seidel, H. *et al*. Widespread genetic incompatibility in C. elegans maintained by balancing selection. *Science* 319, 589-594 (2008).

Thrower, J. *et al*. Recognition of the polyubiquitin proteolytic signal. *EMBO Journal* 19, 94–102 (2000).

Unterholzner, S. *et al*. Toxin–antitoxin systems. *Mobile Genetic Elements* 3, 1-13. (2013).

Wenzel, D. *et al*. UBCH7 reactivity profile reveals parkin and HHARI to be RING/HECT hybrids. *Nature* 474, 105-109 (2011).

Werren, J. *et al.* Selfish genetic elements, genetic conflict, and evolutionary innovation. *PNAS* 108, 10863–10870 (2011).

Wu, F. *et al*. Structural Basis of the Differential Function of the Two C. elegans Atg8 Homologs, LGG-1 and LGG-2, in Autophagy. *Molecular Cell* 60, 914–929 (2015).

Yamaguchi, Y. *et al.* Regulation of growth and death in Escherichia coli by toxin--antitoxin systems. *Nature Reviews Microbiology* 9, 779-790. (2011).

Yuan, L., *et al*. Structural insights into the mechanism and E2 specificity of the RBR E3 ubiquitin ligase HHARI. *Nature Communications* 8, 1-14 (2017).